Isomorphous Substitutions of Calcium with Rare-Earth Elements and Lithium in Scheelite-Structured Molybdates for Actinoid Simulation

E. I. Get'man and S. V. Radio

Vasyl' Stus Donetsk National University,
21, 600-Richchia Str.,
UA-21027 Vinnytsia, Ukraine

Using V. S. Urusov's crystal-energy theory of isomorphous miscibility, the mixing energies, critical decomposition temperatures, and limits of isomorphous substitutions are calculated, and the regions of thermodynamic stability of $Ca_{1-x}(Li_{0.5}Ln_{0.5})_xMoO_4$ solid solutions, where Ln are rare-earth elements (REE), are determined. As shown, the critical decomposition temperatures decrease symbately with the mixing energy as the REE number increases in the La–Sm series within the temperature range of 162–16 K, and it increases in the Eu–Lu series within the temperature range of 30–294 K. The thermodynamic stability diagram and the decomposition domes of solid solutions in the concentration range from $x = 0$ to $x = 1.0$ through $x = 0.05$ are presented. These allow for the determination of equilibrium substitution limits by temperature, temperature by a given substitution limit, or ranges of thermodynamic stability of solid solutions. The results may be useful for the storage and disposal of actinoides, radioactive REE isotopes, and molybdenum in the field of ultra-low temperatures.

З використанням кристалоенергетичної теорії ізоморфної змішуваности В. С. Урусова розраховано енергії змішання, критичні температури розпаду, межі ізоморфних заміщень, а також визначено області термодинамічної стабільности твердих розчинів $Ca_{1-x}(Li_{0.5}Ln_{0.5})_xMoO_4$, де Ln — рідкісноземельні елементи (РЗЕ). Показано, що критичні температури розпаду зі збільшенням номера РЗЕ в ряду La–Sm симбатно з енергією змішання зменшуються в інтервалі температур 162–16 К, а в ряду Eu–Lu зростають в інтервалі температур 30–294 К. Представлено діяграму термодинамічної стабільности, а також бані розпаду твердих розчинів у діяпазоні концентрацій від $x = 0$ до $x = 1,0$ через $x = 0,05$. Вони дають змогу визначати рівноважні межі заміщень за температурою, або температуру за заданою межею заміщення, чи то області термодинамічної стабільности твердих розчинів. Результати роботи можуть бути корис-

ними для зберігання та захоронення актиноїдів, радіоактивних ізотопів РЗЕ та Молібдену в області наднизьких температур.

1. INTRODUCTION

Materials with scheelite mineral structure (calcium tungstate, $CaWO_4$), based on individual molybdates and tungstates or solid solutions, which are considered as matrices for immobilizing radioactive isotopes, can contain elements in oxidation states from +1 to +7 (in the Ca positions: Li, Na, K, Rb, Cs, and Tl; Ca, Sr, Ba, Mn, and Cu; Fe, La–Lu, and Y; Th, U, Np, and Pu; in the W positions: Nb, Ta, Mo, W, Re, I, V, and Ge [1]. Normal salts of tungstates and molybdates of alkaline earth elements of the composition $M^{II}XO_4$ and double molybdates and tungstates of alkali and rare-earth elements (REE) of the composition $Na_{0.5}Ln_{0.5}XO_4$ (where M^{II} is an alkaline earth metal, Ln is a rare-earth element, and $X =$ Mo or W) with a scheelite structure are of interest due to their potential practical applications as ion conductors, microwave dielectrics [2], luminophores [3], scintillators [4], LEDs, optical fibres, photocatalysts for wastewater treatment [5], high-performance electrochemical supercapacitors for energy storage and conversion [6], lasers [7], and in many other cases.

Of particular interest is the recent trend of using molybdates and tungstates of alkaline earth elements doped with double molybdates and tungstates of alkali metals and REEs with a scheelite structure for the storage and disposal of high-level radioactive waste with long-lived radioactivity [8–13]. Previously, alumophosphate or borosilicate glasses, which have a lifetime of no more than 30–40 years, were used as matrices for radioactive waste disposal [14]. According to [8, 15], under conditions typical for deep geological repositories, borosilicate glass may dissolve upon contact with groundwater over geological timescales. Meanwhile, according to current regulations, the matrix material must ensure environmental safety for more than 10^5 years [16]. Such a long time can be provided by ceramic matrices of minerals that can persist in natural conditions for at least the above-mentioned number of years, in partic-

ular, molybdates and tungstates of alkaline-earth elements with a scheelite-type structure, which can isomorphously incorporate radioactive isotopes of actinoides and lanthanides close to them in size and charge (the amount of the latter, according to [17], is up to 35 wt.% of nuclear reactor waste), as well as radioactive isotopes of molybdenum.

However, most publications focus on studying synthesis conditions and properties of the corresponding solid solutions but do not predict their behaviour during storage and disposal. As known [18], solid solutions tend to decompose upon cooling, which can lead to the degradation of materials based on them, as well as changes and non-reproducibility of their properties. The insufficient information on the substitution limits and thermodynamic stability areas of solid solutions forces researchers to choose material compositions and synthesis conditions either by analogy with related systems or by the 'trial and error' method, which can lead to excessive consumption of expensive reagents and increase the duration of research. Therefore, it is rational to apply not only experimental but also computational methods, free from the drawbacks. An example of such an approach can be found in the works [19, 20], where the results of calculations from the study [21] were used to select synthesis conditions for solid solution samples of the $Y_{1-x}Sc_xPO_4$ system.

At the same time, to date, studies have mainly focused on systems in which larger REE ions were used as simulators for large triple-charged actinoides, such as U or Pu, in matrices containing strontium and sodium [9−13]. At the same time, to the best of our knowledge, only in the $Ca_{1-x}Li_{x/2}Gd_{x/2}MoO_4$ system [8] was Gd^{3+} used as a simulator for minor actinoide Cm^{3+}, involving, according to the requirements of isomorphous substitutions [18], smaller calcium and lithium cations compared to strontium and sodium. As noted in Ref. [8], the study of the structure and chemical stability of $Ca_{1-x}Li_{x/2}Gd_{x/2}MoO_4$ yields promising results in the development of new single- or multicomponent systems for immobilizing high-level nuclear waste with high molybdenum content.

Therefore, the present work aimed to predict the limits of isomorphous substitutions and the thermodynamic stability of $Ca_{1-x}(Li_{0.5}Ln_{0.5})_xMoO_4$ solid solutions with a scheelite structure containing REE cations as actinoide simulators for the disposal of high-level radioactive waste.

2. INITIAL DATA AND CALCULATION METHODOLOGY

In V. S. Urusov's crystal-energy theory of isomorphous miscibility, the main problem in determining the limits of isomorphous substitutions is finding the mixing energy (Q_{mix}) [18]. Since both compo-

nents of the $Ca_{1-x}(Li_{0.5}Ln_{0.5})_xMoO_4$ systems are isostructural with scheelite, the mixing energy can be calculated as the sum of only two contributions, resulting from the differences in the degrees of ionicity of the chemical bonds in the system components (Q_ε) and the sizes of the substituting structural units (Q_R) [18]:

$$Q_{mix} = Q_\varepsilon + Q_R = \frac{1390 m z_m z_x \alpha (\Delta\varepsilon)^2}{2R} + C m n z_m z_x \left(\frac{\Delta R}{R_1}\right)^2 \text{ [kJ/mol]}, (1)$$

where $m = 2$ is the number of different structural units in the components of the systems in the pseudobinary approximation of the scheelite structure (lithium and lanthanides, statistically located at the cation sites in the $Li_{0.5}Ln_{0.5}MoO_4$ scheelite structure, are considered as one structural unit, and the molybdate anion is considered as the second one); $z_m = z_x = 2$—the formal (integer) charges of the substituting (z_m) and common (z_x) structural units of the components; $\alpha = 1.723$ is the reduced Madelung constant, calculated using the Templeton formula [22]; $C = 20(2\Delta\chi + 1)$ is a constant depending on the properties of the components, where $\Delta\chi$ is the difference in electronegativity (χ) values of the cations taken from Ref. [23], and the anion MoO_4^{2-} taken, according to the recommendation [24], as equal to the χ of the oxide anion O^{2-} (3.758). The choice of the χ scale [23], as opposed to the scales of other authors, was because the χ values change in it with a regular periodicity, increasing in the series $La^{3+}-Eu^{3+}$ from 1.327 to 1.433 and $Gd^{3+}-Yb^{3+}$ from 1.386 to 1.479, with a sharp drop during the transitions $Eu^{3+}-Gd^{3+}$ from 1.433 to 1.386 and $Yb^{3+}-Lu^{3+}$ from 1.479 to 1.431, which is due to the structure of the electronic shells of the REEs. Europium and gadolinium have a half-filled $4f$-shell (7 electrons), and ytterbium and lutetium have a filled shell (14 electrons). When transitioning from europium to gadolinium and from ytterbium to lutetium, the first electron appears in the $5d$-sublevel; $n = 8$ is co-ordination number of the substituting structural unit in the pseudobinary representation of the scheelite structure; $R_{Li, Ln-M}$ is interatomic distance 'cation−tetrahedral anion' in $Li_{0.5}Ln_{0.5}MoO_4$ calculated from the unit cell parameters taken from Ref. [25]; ΔR is the difference in the interatomic distances 'cation−tetrahedral anion' in $CaMoO_4$ and $Li_{0.5}Ln_{0.5}MoO_4$; $\Delta R/R_1$ is relative difference in the interatomic distances 'cation−tetrahedral anion' in the system components (dimensional parameter); R_1 is interatomic distance 'cation−tetrahedral anion' in the system component with the smaller cation radius; $\Delta\varepsilon$ is the difference in the degrees of ionicity of the chemical bonds in the system components in the pseudobinary approximation of the structure. The degree of ionicity of the chemical bond ε in the crystals was determined by the difference in χ between the tetrahedral

TABLE 1. Some initial data[*], calculated mixing energies, and critical decomposition temperatures of the solid solutions in the $Ca_{1-x}(Li_{0.5}Ln_{0.5})_xMoO_4$ systems.

Ln	$R(LiLn(MoO_4)_2)$, Å	χ_{Ln}	$\Delta\chi$	$C = 20\cdot(2\Delta\chi + 1)$	$\Delta R/R_1$	Q_R, kJ/mole	Q_{mix}, kJ/mole	T_{cr}, K
La	3.851	1.327	2.594	123.76	0.0185	2.710	2.720	162
Ce	3.837	1.348	2.589	123.56	0.0148	1.732	1.772	105
Pr	3.812	1.374	2.582	123.28	0.0081	0.518	0.609	36
Nd	3.798	1.382	2.580	123.2	0.0044	0.153	0.314	19
Sm	3.775	1.410	2.573	122.92	0.0016	0.020	0.274	16
Eu	3.765	1.433	2.567	122.68	0.0043	0.145	0.511	30
Gd	3.756	1.386	2.579	123.16	0.0067	0.359	0.522	31
Tb	3.744	1.410	2.573	122.92	0.0099	0.771	1.027	61
Dy	3.734	1.426	2.569	122.76	0.0126	1.249	1.618	96
Ho	3.727	1.433	2.567	122.68	0.0145	1.651	2.021	120
Er	3.714	1.438	2.566	122.64	0.0181	2.571	3.077	183
Tm	3.707	1.455	2.562	122.48	0.0200	3.135	3.642	217
Yb	3.698	1.479	2.556	122.24	0.0225	3.961	4.800	286
Lu	3.692	1.431	2.568	122.72	0.0241	4.562	4.936	294

[*]*Note:* The unit cell parameters of $CaMoO_4$ for calculating the distance $R(CaMoO_4) = 3.7812$ Å are taken from Ref. [30], and the distances $R(LiLn(MoO_4)_2)$ are taken from Ref. [31]. $\chi_{Li} = 1.009$; $\chi_{Ca} = 1.160$; $\chi(Ca_{1-x}(Li_{0.5}Ln_{0.5})_x) = ((\chi_{Li} + \chi_{Ln})/2 + \chi_{Ca})/2$; $\Delta\chi = 3.758 - ((\chi_{Li} + \chi_{Ln})/2 + \chi_{Ca})/2$.

anion and the cations according to the tabulated data provided by S. Batsanov [26].

Since the size parameter, $\Delta R/R_1$, was significantly less than 0.1 (Table 1), according to Ref. [18], the calculation of the equilibrium substitution limits as a function of temperature was carried out in the approximation of regular solid solutions using Becker's equation [27]

$$\frac{-(1-2x)}{\ln\left[x/(1-x)\right]} = \frac{R_g T_d}{Q_{mix}}, \qquad (2)$$

where x is the mole fraction of the dissolved component, R_g is the universal gas constant, T_d is the decomposition temperature of the

solid solution. The values of R_g and Q_{mix} in both latter cases were expressed in calories [18].

The critical decomposition temperatures, T_{cr}, were calculated according to Ref. [18] in the approximation of regular solid solutions using equation

$$T_{cr} = \frac{Q_{mix}}{2kN},\qquad(3)$$

where k is the Boltzmann constant, and N is the Avogadro number.

The error in calculating the critical (maximum) decomposition temperature of solid solutions was ±100 K, and the mixing energy Q_R, considering the error of the initial data, was up to $\pm13\%$ [18].

3. RESULTS OF CALCULATIONS AND THEIR DISCUSSION

3.1. Mixing Energies of Solid Solutions

Some initial data and calculation results of mixing energies are summarized in Tables 1 and 2 and presented in Fig. 1. As can be

TABLE 2. Data for calculating the mixing energy for solid solutions in the $Ca_{1-x}(Li_{0.5}Ln_{0.5})_xMoO_4$ systems.

Ln	$\chi(MoO_4) - \chi(Li_{0.5}Ln_{0.5})$	$\varepsilon(Li_{0.5}Ln_{0.5})MoO_4$	$\Delta\varepsilon^*$	Q_ε, kJ/mole
La	2.590	0.768	0.002	0.010
Ce	2.579	0.766	0.004	0.040
Pr	2.566	0.764	0.006	0.091
Nd	2.562	0.762	0.008	0.161
Sm	2.548	0.760	0.010	0.254
Eu	2.537	0.758	0.012	0.366
Gd	2.560	0.762	0.008	0.163
Tb	2.548	0.760	0.010	0.256
Dy	2.540	0.758	0.012	0.369
Ho	2.537	0.758	0.012	0.370
Er	2.534	0.756	0.014	0.506
Tm	2.526	0.756	0.014	0.507
Yb	2.514	0.752	0.018	0.839
Lu	2.538	0.758	0.012	0.374

Note: $\Delta\varepsilon = \varepsilon(CaMoO_4) - \varepsilon(Li_{0.5}Ln_{0.5})MoO_4$; the value of $\varepsilon(CaMoO_4) = 0.77$ was determined according to the tabular data of S. Batsanov [26], based on $\chi(MoO_4) = 3.758$ and $\chi(Ca) = 1.160$.

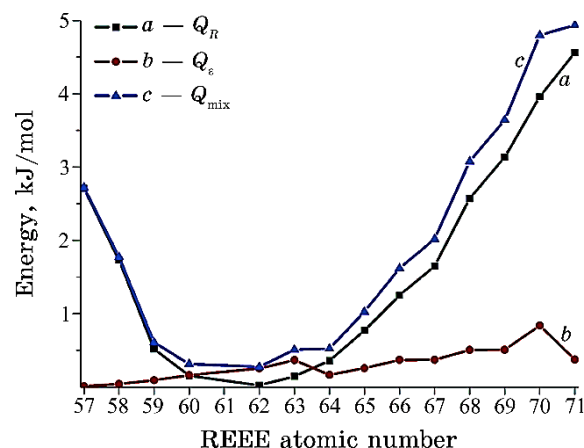**Fig. 1.** Dependences of the calculated contributions to the mixing energy Q_R (*a*), Q_ε (*b*), and the total mixing energy Q_{mix} (*c*) of the $Ca_{1-x}(Li_{0.5}Ln_{0.5})_xMoO_4$ systems on REE atomic number.

seen from the data provided, with an increase in the atomic number of REEs, the contributions to the total mixing energy due to differences in the sizes of the substituting structural units, Q_R, initially decrease significantly and smoothly from 2.71 to 0.02 kJ/mole in the REEs series from La to Sm, then increase from 0.02 to 4.56 kJ/mole in the REEs series from Sm to Lu (Table 1, Fig. 1 *a*). This is related to a similar change in the size parameter $\Delta R/R_1$, which first decreases from 0.0185 to 0.0044 and then increases to 0.0241. Such a change in $\Delta R/R_1$ is because the crystal ionic radius of the substituted double-charged calcium cation, which mainly determines the value of $\Delta R/R_1$, lies within the range of ionic radii of the substituting REEs from lanthanum to lutetium and is close to the ionic radius of samarium [28].

The dependences of the contributions to the total mixing energy due to differences in the degrees of ionicity of the chemical bonds of the components, Q_ε, for the cerium and yttrium subgroups are identical (Fig. 1, *b*). They systematically increase in the groups of systems containing REEs of the La−Eu series from 0.010 to 0.366 kJ/mole and REEs of the Tb−Yb series from 0.256 to 0.839 kJ/mole, followed by a sharp decrease when transitioning from the system containing Eu to the system containing Gd, from 0.366 to 0.163 kJ/mole, and from the system containing Yb to the system containing Lu, from 0.839 to 0.374 kJ/mol. This is due to the aforementioned structure of the electron shells of the REEs.

According to Ref. [18], in general case, if the differences in the degrees of ionicity of the chemical bonds in the system components

are less than 0.05, the value of Q_ε will be insignificant and can be neglected. This is also because the errors in the values of electronegativity, which served as the basis for calculating Q_ε, are on the order of 0.05 [29], which is much larger than the inaccuracies in determining the parameters of the unit cells, which are mainly used to determine the Q_R energy.

In this case, $\Delta\varepsilon$ varies from 0.002 to 0.018 (Table 2), and most of the Q_ε values are significantly smaller than Q_R (Fig. 1, *a*, *b*). However, in the case of systems with samarium and europium compounds, the Q_ε values, on the contrary, exceed Q_R values. Therefore, the contributions of Q_ε to the mixing energies were considered in all systems.

3.2. Decomposition Temperatures of Solid Solutions

The calculated critical decomposition temperatures T_{cr} of the unlimited series of solid solutions in the $Ca_{1-x}(Li_{0.5}Ln_{0.5})_xMoO_4$ systems (Table 1, Fig. 2, *e* for $x = 0.5$) decrease in the range of 162–16 K with an increasing of REEs atomic number in the La–Sm series, in correlation with the mixing energy. In the Eu–Lu series, the values of T_{cr} increase in the range of 30–294 K. It should be noted that the $Ca_{1-x}(Li_{0.5}Ln_{0.5})_xMoO_4$ systems are characterized by very low critical decomposition temperatures for solid solutions (for 12 out of 14 systems, they are below room temperature), and only for two of
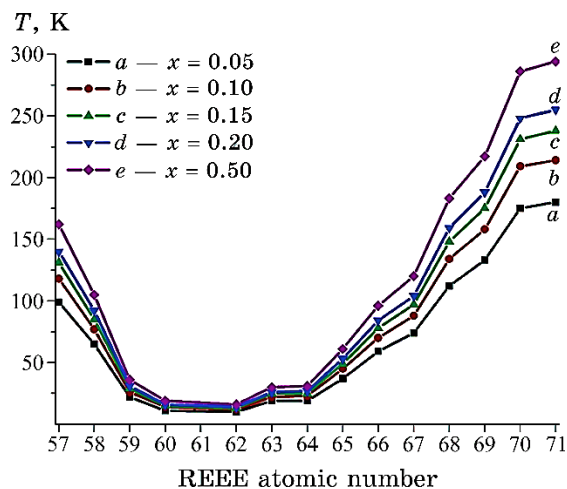

Fig. 2. Dependences of decomposition temperatures for solid solutions in the $Ca_{1-x}(Li_{0.5}Ln_{0.5})_xMoO_4$ systems on the REEs' atomic numbers (thermodynamic-stability diagram) for substitution limits of $x = 0.05$ (*a*), 0.10 (*b*), 0.15 (*c*), 0.20 (*d*), and 0.50 (*e*).

TABLE 3. Calculated thermodynamically possible decomposition temperatures (T_d [K]) for solid solutions in the $Ca_{1-x}(Li_{0.5}Ln_{0.5})_xMoO_4$ systems at $x = 0.05$, 0.10, 0.15, and 0.20.

Ln	Values of T_d [K] at corresponding x			
	0.05	0.10	0.15	0.20
La	99	118	131	140
Ce	65	77	85	92
Pr	22	26	29	31
Nd	11	14	15	16
Sm	10	12	13	14
Eu	19	22	25	26
Gd	19	23	25	27
Tb	37	45	49	53
Dy	59	70	78	84
Ho	74	88	97	104
Er	112	134	148	159
Tm	133	158	175	188
Yb	175	209	231	248
Lu	180	214	238	255

them, $Ca_{1-x}(Li_{0.5}Yb_{0.5})_xMoO_4$ and $Ca_{1-x}(Li_{0.5}Lu_{0.5})_xMoO_4$, they are close to room temperature.

For all systems, based on the critical decomposition temperatures T_{cr} (at $x = 0.5$, Table 1) and the decomposition temperatures (T_d for substitution limits $x = 0.05$, 0.10, 0.15, and 0.20, Table 3) of the limited series of $Ca_{1-x}(Li_{0.5}Ln_{0.5})_xMoO_4$ solid solutions, thermodynamic-stability diagrams, *i.e.*, dependences of decomposition temperatures on the REEs' atomic numbers, have been plotted (Fig. 2).

These dependences can be used to determine graphically the equilibrium substitution limits x at given decomposition temperatures T_d or the decomposition temperatures at given substitution limits [32]. The intersection points of an isotherm, drawn from a given decomposition temperature, with a vertical line drawn from the REE atomic number, make it possible to determine the composition range in which the substitution limit is located. Interpolating the segment of this vertical line between the two nearest curves provides the possible substitution limit.

3.3. Areas of Thermodynamic Stability

From the thermodynamic stability diagram, it follows that the unlimited solid solutions of the $Ca_{1-x}(Li_{0.5}Ln_{0.5})_xMoO_4$ systems, which are

stable at temperatures above the critical (Fig. 2, above curve e), should decompose when the temperature is lowered below the critical, forming limited areas. This would occur if the diffusion rate and time were sufficiently large to allow stable nuclei of the new phase to form and begin to grow.

For each of the $Ca_{1-x}(Li_{0.5}Ln_{0.5})_xMoO_4$ systems, the decomposition temperatures of the solid solutions were calculated in the composition range of $1.0 > x > 0$ with a step of $x = 0.05$ and decomposition domes were plotted (Fig. 3). According to them with greater accuracy than in Fig. 2, it is possible to determine graphically for each system the decomposition temperature at a given substitution limit or the equilibrium substitution limit at a given temperature, as well as the regions of thermodynamic stability. Above the peaks of the decomposition domes, a continuous series of stable solid solutions will exist; below the peaks but above the dome lines, there will be
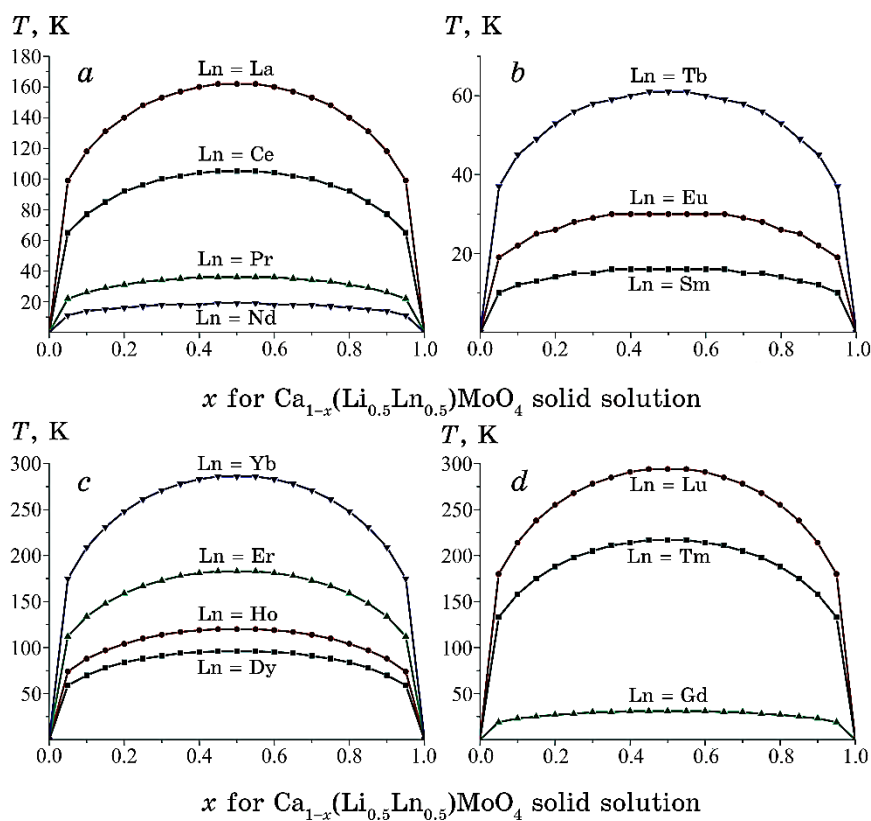

Fig. 3. Decomposition domes for solid solutions in the $Ca_{1-x}(Li_{0.5}Ln_{0.5})_xMoO_4$ $(1.0 > x > 0)$ systems: (a) Ln = La, Ce, Pr, and Nd; (b) Ln = Sm, Eu, and Tb; (c) Ln = Dy, Ho, Er, and Yb; (d) Ln = Gd, Tm, and Lu.

two limited solubility regions; and below the dome lines, there will be two limited solubility regions and mixtures of two solid solutions based on each of the system components.

3.4. Comparison of Calculation Results with Literature Data

As far as we know, there is no literature data on the critical decomposition temperatures, limits of isomorphous substitutions in the case of limited solubility of components, and thermodynamic stability of solid solutions in the $Ca_{1-x}(Li_{0.5}Ln_{0.5})_xMoO_4$ systems.

Previously (see Table 3), the synthesis conditions and some properties of solid solutions in systems with wide areas of solid solutions, such as $[(Li_{0.5}Nd_{0.5})_{1-x}Ca_x]MoO_4$ and $[(Li_{0.5}Sm_{0.5})_{1-x}Ca_x]MoO_4$ ($x = 0.2-0.9$) [33], the unlimited solubility of components in $Ca_{1-2x}Eu_xLi_xMoO_4$ [34] and $[(Li_{0.5}Gd_{0.5})_{1-x}Ca_x]MoO_4$ [8], as well as one solid solution composition $Ca_{0.9}MoO_4$:$0.05Eu^{3+}$, $0.05Li^+$ [35], have been studied. Additionally, the literature presents results on the study of solid solutions in the systems $CaMoO_4$:Eu^{3+}, Li^+ [36] and $CaMoO_4$:Eu^{3+}, M^+ ($M = Li$, Na, K) [37] without specifying the component ratios.

The results obtained in this study are consistent with the data [8, 33–37] in the sense that the synthesis temperature ranges for the samples of these systems (673–1223 K, Table 3) fall within the predicted areas of thermodynamic stability of the solid solutions, *i.e.*, well above the decomposition domes presented in Fig. 3, *a*, *b*, and *d*.

It is known [38] that, for radioactive waste disposal, its components are included in chemically and mechanically stable matrices, with subsequent placement in underground storage until the complete decay of radionuclides or until their activity approaches the level of the surrounding natural background. In this process, the oxides of fission products are incorporated into a glassy matrix, since glass, being a non-stoichiometric compound, can dissolve a complex mixture of fission products in its liquid state and subsequently retain it firmly upon cooling (and solidification). The resulting product has relatively high chemical and radiation resistance. Most commonly, two types of glass are widely used for immobilizing radioactive waste: aluminophosphate glass and borosilicate glass. However, the main problem of glass remains unresolved, *i.e.*, its thermodynamic instability, which manifests as glass crystallization (devitrification) under the influence of increased temperatures caused by radioactive decay. Devitrification phenomena degrade the initial properties of the product, particularly increasing its leaching rate, resulting in the release of radioactive waste elements into the solution over a relatively short period. In addition, due to the formation of crystalline phases with a total lower iso-

morphous capacity than that of glass, some radionuclides may leach into aqueous solutions, posing a threat to the biosphere. It is noted [39] that glass and ceramics are among the most reliable materials for immobilizing radioactive waste. Ceramic matrices have the greatest potential for practical use due to their high chemical stability and thermal stability. Ceramics based on natural and artificially synthesized mineral additives can incorporate a significantly larger volume of radioactive waste than glass. Furthermore, it has been noted [40] that the immobilization of certain radioactive isotopes proves to be a more complex process for molybdenum-rich waste generated during the reprocessing of used nuclear fuel, such as UMo−MoSnAl fuel from gas-graphite reactors, or mixed waste containing lanthanides and transition metals proposed for nuclear fuel reprocessing in the United States. In both cases, immobilization in glass is found to be impossible, as the waste contains substantial amounts of highly radioactive isotopes that release heat during decay, as well as a large quantity of molybdenum that exceeds the solubility limits in borosilicate glasses. Currently, it is planned to mix such waste with aluminoborosilicate, during which separation into two liquid phases occurs upon cooling, followed by the crystallization of molybdate phases and further additional separation into two liquid phases. It has been noted [40] that a detailed understanding of the thermochemistry of vitrification and phase formation processes is required to ensure the formation of the desired crystalline phase.

As the further development of nuclear power engineering could lead to unacceptable radioactive contamination of the Earth's biosphere, one direction for preventing this situation could be the disposal of radioactive waste in space [41]. If it becomes necessary to dispose of radioactive waste not only within the Earth's crust but also at ultra-low temperatures in space, materials based on solid solutions of $Ca_{1-x}(Li_{0.5}Ln_{0.5})_xMoO_4$ may be used, particularly those containing Nd, Sm, Eu, Gd, and actinoides close to them in size. Such materials have lower critical decomposition temperatures (16−31 K) compared to previously recommended materials based on solid solutions of other compositions: phosphates $La_{1-x}Ln_xPO_4$, fluorides $La_{1-x}Ln_xF_3$, and arsenates $Lu_{1-x}Ln_xAsO_4$. The critical decomposition temperatures of the latter are in the intervals of 150−830 K [42], 522−1811 K [43], and 186−624 K [44], respectively.

4. CONCLUSIONS

1. Within the framework of V. S. Urusov's crystal-energy theory of isomorphous substitutions, the mixing energies (interaction parameters), critical decomposition (stability) temperatures, and the lim-

its of isomorphous substitutions have been calculated, and the thermodynamic stability of the solid solutions in the $Ca_{1-x}(Li_{0.5}Ln_{0.5})_xMoO_4$ systems, where Ln are rare earth elements, has been assessed.

2. It has been shown that with the increase in the REE number, the contributions to the total mixing energy due to differences in the sizes of the substituting structural units, Q_R, initially decrease significantly from 2.71 to 0.02 kJ/mole in the REEs series from La to Sm, and then increase from 0.02 to 4.56 kJ/mole in the REEs' series from Sm to Lu.

3. The contributions to the total mixing energy Q_{mix} due to differences in the sizes of the substituting structural units Q_R significantly exceed the contributions due to differences in the degrees of ionicity of the components Q_ε. However, in the case of systems with samarium and europium compounds, the Q_ε values exceed the Q_R values.

4. The calculated critical decomposition temperatures T_{cr} of the unlimited series of solid solutions in the studied systems decrease along with the mixing energy as the REEs' numbers increase in the La−Sm series, ranging from 162 to 16 K, and increase in the Eu−Lu series, ranging from 30 to 294 K.

5. A thermodynamic stability diagram and decomposition domes for each solid solution system are presented in the concentration range from $x = 0$ to $x = 1.0$ through $x = 0.05$. These allow for the graphical determination of the decomposition temperature of solid solutions for a given composition x, the equilibrium substitution limit for a given decomposition temperature, and the assessment of thermodynamic stability regions over a wide range of compositions and temperatures.

6. The calculated results do not contradict the literature data, in the sense that the temperature range for obtaining samples of previously synthesized systems falls within the thermodynamic stability regions of solid solutions as predicted by modelling.

7. For the disposal of radioactive waste at extremely low temperatures (*e.g.*, in space), materials based on solid solutions of $Ca_{1-x}(Li_{0.5}Ln_{0.5})_xMoO_4$, particularly those containing Nd, Sm, Eu, Gd, and actinoides of similar size, may be used. These materials have significantly lower critical decomposition temperatures (16−31 K) compared to previously recommended materials based on solid solutions of other compositions such as $La_{1-x}Ln_xPO_4$ phosphates, $La_{1-x}Ln_xF_3$ fluorides, and $Lu_{1-x}Ln_xAsO_4$ arsenates.

ACKNOWLEDGMENTS

REFERENCES

1.   A. I. Orlova and M. I. Ojovan, *Materials*, **12**: 2638 (2019); https://doi.org/10.3390/ma12162638
2.   A. A. Nikitina, Z. A. Mikhaylovskaya, N. S. Knyazev, A. I. Malkin, and A. N. Korotkov, *Fizika. Tekhnologii. Innovatsii: Sbornik Statey VII Mezhdunarodnoy Molodezhnoy Nauchnoy Konferentsii* (Yekaterinburg: UrFU: 2020) (in Russian); http://elar.urfu.ru/handle/10995/91850
3.   I. C. Nogueira, L. S. Cavalcante, P. F. S. Pereira, M. M. de Jesus, J. M. Rivas Mercury, N. C. Batista, M. Siu Li, and E. Longo, *J. Appl. Cryst.*, **46**, No. 5: 1434 (2013); https://doi.org/10.1107/S0021889813020335
4.   A. Priya, E. Sinha, and S. K. Rout, *Solid State Sci.*, **20**: 40 (2013); https://doi.org/10.1016/j.solidstatesciences.2013.03.002
5.   B. Bakiz, A. Hallaoui, A. Taoufyq, A. Benlhachemi, F. Guinneton, S. Villain, M. Ezahri, J.-C. Valmalette, M. Arab, and J.-R. Gavarri, *J. Solid State Chem.*, **258**: 146 (2018); https://doi.org/10.1016/j.jssc.2017.10.014
6.   T. Anitha, A. E. Reddy, Y. A. Kumar, Y.-R. Cho, and H.-J. Kim, *Dalton Trans.*, **48**, No. 28: 10652 (2019); https://doi.org/10.1039/C9DT01931F
7.   O. A. Buryi, D. M. Vynnyk, T. I. Voroniak, I. V. Stasyshyn, A. T. Ratych, and A. S. Andrushchak, *Ukrainian Journal of Physics*, **68**, No. 2: 92 (2023); https://doi.org/10.15407/ujpe68.2.92
8.   Ch. Meng, W. Li, Ch. Ren, and J. Zhao, *J. Mater. Sci.*, **55**: 2741 (2020); https://doi.org/10.1007/s10853-019-04223-y
9.   M. G. Tokarev, E. A. Potanina, A. I. Orlova, S. A. Khainakov, M. S. Boldin, E. A. Lantsev, N. V. Sakharov, A. A. Murashov, S. Garcia-Granda, A. V. Nokhrin, and V. N. Chuvil'deev, *Inorg. Mater.*, **55**, No. 7: 730 (2019); https://doi.org/10.1134/S0020168519070203
10.   A. I. Orlova, Ye. A. Potanina, M. G. Tokarev, M. S. Boldin, and Ye. A. Lantsev, *Voprosy Radiatsionnoy Bezopasnosti*, **2**, No. 86: 2 (2017) (in Russian).
11.   E. A. Potanina, A. I. Orlova, D. A. Mikhailov, A. V. Nokhrin, V. N. Chuvil'deev, M. S. Boldin, N. V. Sakharov, E. A. Lantcev, M. G. Tokarev, and A. A. Murashov, *J. Alloy Compd.*, **774**: 182 (2019); https://doi.org/10.1016/j.jallcom.2018.09.348
12.   E. A. Potanina, A. I. Orlova, A. V. Nokhrin, M. S. Boldin, N. V. Sakharov, O. A. Belkin, V. N. Chuvil'deev, M. G. Tokarev, S. V. Shotin, and A. Yu. Zelenov, *Ceram. Int.*, **44**, No. 4: 4033 (2018); https://doi.org/10.1016/j.ceramint.2017.11.199
13.   A. A. Belov, O. O. Shichalin, E. K. Papynov, I. Y. Buravlev, A. S. Portnyagin, S. A. Azon, A. N. Fedorets, A. A. Vornovskikh, E. S. Kolodeznikov, E. A. Gridasova, A. Pogodaev, N. B. Kondrikov, Y. Shi, and I. G. Tananaev, *Materials*, **16**, No. 17: 5838 (2023); https://doi.org/10.3390/ma16175838
14.   A. E. Grechanovsky, N. N. Eremin, and V. S. Urusov, *Phys. Solid State*, **55**, No. 9: 1929 (2013); https://doi.org/10.1134/S1063783413090138

15.   D. Bosbach, T. Rabung, F. Brandt, and T. Fanghänel, *Radiochim. Acta*, **92**, Nos. 9−11: 639 (2004); https://doi.org/10.1524/ract.92.9.639.54976

16.   I. S. Skiter and Ye. Ye. Vtornikova, *Yaderna ta Radiatsiyna Bezpeka* [Nuclear and Radiation Safety], **2**, No. 78: 36 (2018) (in Ukrainian); https://doi.org/10.32918/nrs.2018.2(78).06

17.   L. A. Boatner, *Rev. Mineral. Geochem.*, **48**, No. 1: 87 (2002); https://doi.org/10.2138/rmg.2002.48.4

18.   V. S. Urusov, *Teoriia Izomorfnoi Smesimosti* [The Theory of Isomorphous Miscibility] (Moskva: Nauka: 1977) (in Russian).

19.   D. Spassky, A. Vasil'ev, V. Nagirnyi, I. Kudryavtseva, D. Deyneko, I. Nikiforov, I. Kondratyev, and B. Zadneprovski, *Materials*, **15**, No. 19: 6844 (2022); https://doi.org/10.3390/ma15196844

20.   V. S. Voznyak-Levushkina, A. A. Arapova, D. A. Spassky, I. V. Nikiforov, and B. I. Zadneprovski, *Phys. Solid State*, **64**, No. 11: 567 (2022); https://doi.org/10.1134/S1063783422110130

21.   E. I. Get'man, S. V. Radio, and L. I. Ardanova, *Inorg. Mater.*, **54**, No. 6: 596 (2018); https://doi.org/10.1134/S0020168518060031

22.   D. H. Templeton, *J. Chem. Phys.*, **21**, No. 11: 2097 (1953); https://doi.org/10.1063/1.1698788

23.   K. Li and D. Xue, *J. Phys. Chem. A*, **110**, No. 39: 11332 (2006); https://doi.org/10.1021/jp062886k

24.   S. S. Batsanov, *Russ. Chem. Rev.*, **37**, No. 5: 332 (1968); https://doi.org/10.1070/RC1968v037n05ABEH001639

25.   A. A. Yevdokimov, V. A. Yefremov, V. K. Trunov, I. A. Kleyman, and B. F. Dzhurinskiy, *Soyedineniya Redkozemel'nykh Ehlementov. Molibdaty, Vol'framaty* [Compounds of Rare-Earth Elements. Molybdates, Tungstates] (Moskva: Nauka: 1991) (in Russian).

26.   S. S. Batsanov, *Strukturnaya Khimiya. Fakty i Zavisimosti* [Structural Chemistry. Facts and Dependences] (Moskva: Dialog-MGU: 2000) (in Russian).

27.   R. Becker, *Z. Metallkd.*, **29**: 245 (1937).

28.   R. D. Shannon, *Acta Crystallogr., Sect. A*, **32**, No. 5: 751 (1976); https://doi.org/10.1107/S0567739476001551

29.   L. Pauling, *General Chemistry* (San-Francisco: W. H. Freeman and Co.: 1970).

30.   E. Gürmen, E. Daniels, and J. S. King, *J. Chem. Phys.*, **55**, No. 3: 1093 (1971); https://doi.org/10.1063/1.1676191

31.   E. I. Get'man, *Izomorfnyye Zameshcheniya v Vol'framatnykh i Molibdatnykh Sistemakh* [Isomorphous Substitutions in Tungstate and Molybdate Systems] (Novosibirsk: Nauka: 1985) (in Russian).

32.   E. I. Get'man, S. V. Radio, L. B. Ignatova, and L. I. Ardanova, *Russ. J. Inorg. Chem.*, **64**, No. 1: 118 (2019); https://doi.org/10.1134/S0036023619010091

33.   H.-H. Xi, D. Zhou, H.-D. Xie, B. He, and Q.-P. Wang, *J. Am. Ceram. Soc.*, **98**, No. 2: 587 (2015); https://doi.org/10.1111/jace.13332

34.   J. Wang, X. Jing, Ch. Yan, and J. Li, *J. Electrochem. Soc.*, **152**, No. 3: G186 (2005); https://doi.org/10.1149/1.1856924

35.   Q. Zhang and Zh. Xia, *RSC Adv.*, **4**, No. 95: 53237 (2014); https://doi.org/10.1039/C4RA09136A

36. X. Wang, Y. He, G. Peng, Zh. Liang, and J. Wu, *Chinese Journal of Materials Research*, **26**, No. 6: 615 (2012); https://www.cjmr.org/EN/Y2012/V26/I6/615

37. X. Liu, L. Li, H. M. Noh, J. H. Jeong, K. Jang, and D. S. Shin, *RSC Adv.*, **5**, No. 13: 9441 (2015); https://doi.org/10.1039/C4RA12183J

38. A. R. Kotelnikov, G. M. Akhmedzhanova, N. I. Suk, K. V. Martynov, O. T. Gavlina, and V. A. Suvorova, *Geochem. Int.*, **57**, No. 10: 1066 (2019); https://doi.org/10.1134/S0016702919100057

39. O. E. Shubabko, G. Ye. Ovsyannikova, Min Kheyn Tkhet, and M. A. Vartanyan, *Uspekhi v Khimii i Khimicheskoy Tekhnologii*, **32**, No. 2: 188 (2017) (in Russian).

40. J. S. McCloy and A. Goel, *MRS Bulletin*, **42**: 233 (2017); https://doi.org/10.1557/mrs.2017.8

41. A. V. Degtyarev, *Kosmichna Nauka i Tekhnologiya*, **20**, No. 1: 58 (2014); https://www.mao.kiev.ua/biblio/jscans/knit/2014-20/knit-2014-20-1-07-degtyarev.pdf

42. E. I. Get'man and S. V. Radio, *Inorg. Mater.*, **53**, No. 7: 718 (2017); https://doi.org/10.1134/S0020168517070044

43. Y. A. Oleksii, E. I. Get'man, S. V. Radio, L. I. Ardanova, and E. E. Zubov, *2021 IEEE 11ᵗʰ International Conference 'Nanomaterials: Applications & Properties' (NAP) (Odesa, Ukraine, 2021)*, p. 1–5; https://doi.org/10.1109/NAP51885.2021.9568596

44. E. I. Get'man, Y. A. Oleksii, O. V. Kudryk, S. V. Radio, and L. I. Ardanova, *Nanomaterials and Nanocomposites, Nanostructure Surfaces, and Their Applications. Springer Proceedings in Physics* (Eds. O. Fesenko and L. Yatsenko) (Cham: Springer: 2021), vol. **263**, p. 3; https://doi.org/10.1007/978-3-030-74741-1_1